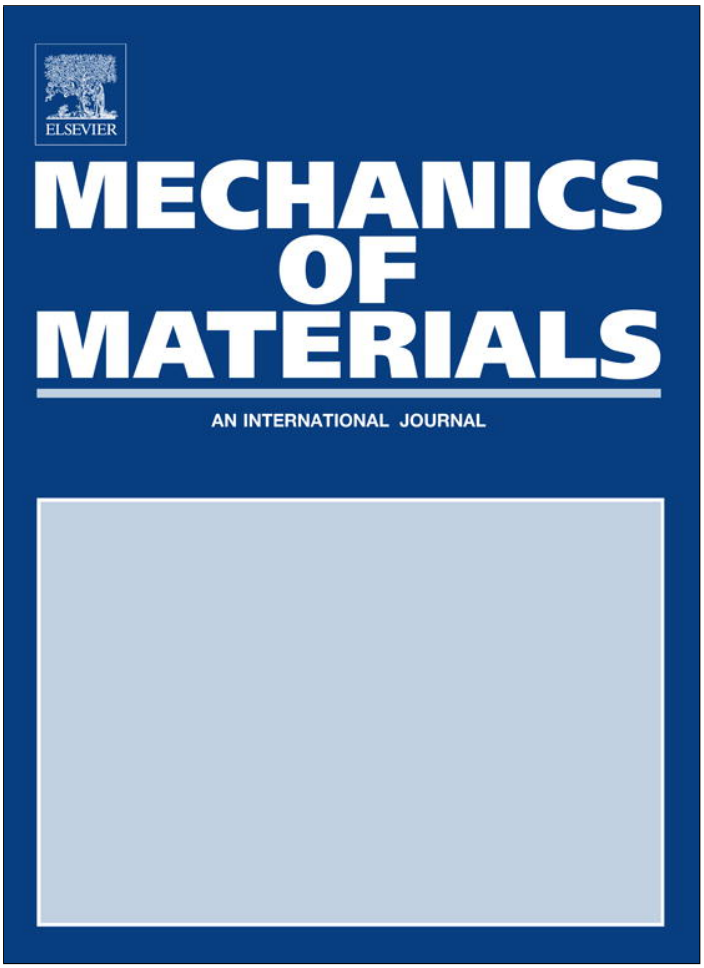

(This is a sample cover image for this issue. The actual cover is not yet available at this time.)

Mechanics of Materials 55 (2012) 41–48

Contents lists available at SciVerse ScienceDirect

Mechanics of Materials

journal homepage: www.elsevier.com/locate/mechmat

Effects of interfacial excess energy on the elastic field of a nano-inhomogeneity

Xujun Zhao [a], Jianmin Qu [a,b,*]

[a] Department of Mechanical Engineering, Northwestern University, Evanston, IL 60208, USA
[b] Department of Civil and Environmental Engineering, Northwestern University, Evanston, IL 60208, USA

ARTICLE INFO

Article history:
Received 4 December 2011
Received in revised form 31 May 2012
Available online 9 August 2012

Keywords:
Variational principle
Nano-inhomogeneity
Interface elasticity
Anisotropic solids

ABSTRACT

A semi-analytical approach based on a variational framework is developed to obtain the three-dimensional solution for a nano-scale inhomogeneity with arbitrary eigenstrains embedded in a matrix of infinite extent. Both the inhomogeneity and the matrix can be elastically anisotropic. The Gurtin–Murdoch surface/interface model is used to describe the elastic behavior of the inhomogeneity/matrix interface. The displacement fields in the inhomogeneity and the matrix are represented, respectively, by two sets of polynomials. Coefficients of these polynomials are determined by solving a system of linear algebraic equations that are derived from minimizing the total potential energy of the system. In the case of an isotropic spherical inhomogeneity with dilatational eigenstrain in an isotropic matrix, our solution shows an excellent agreement with the corresponding analytical solution available in the literature. To demonstrate the capabilities of the method developed here and to investigate the effect of interfacial excess energy, numerical examples are also presented when the inhomogeneity and matrix are both elastically anisotropic. Both dilatational and pure shear eigenstrains are considered in these examples.

1. Introduction

Nanostructured materials, e.g., polycrystalline solids with nano-scale grains, and high temperature superalloys with nano-scale precipitates, exhibit many unique properties not seen in conventional materials, such as high strength and ductility. To a large extent, these unique characteristics are attributed to the extraordinarily high interface to volume ratio in these nanostructured materials (Ashby et al., 2009). Generally speaking, atoms near a surface or an interface have different electronic density from atoms in the bulk (Daw et al., 1993). Consequently, the energy associated with atoms near the surface or interface is different from these in the bulk. The influence of these surface/interface atoms is much more pronounced in nanostructured materials because of their high interface to volume ratio.

In traditional continuum mechanics, the surface/interface energy is generally neglected. To account for the interfaces, Gurtin and Murdoch (1975) and Gurtin et al. (1998) developed a mathematical continuum framework in which the effects of surface/interfaces are accounted for by introducing the interfacial stress. Recently, this general framework has been used by a number of researchers to study the behavior of nanostructured materials. For example, He and Lilley (2008) examined the influence of surface stress effect on the bending resonance of nanowires with different boundary conditions. Dingreville et al. (2005) studied the effective modulus of nano-wires, nano-dots and nano-films. Zhao and Rajapakse (2009) investigated surface energy effects on the elastic field of an isotropic elastic layer bonded to a rigid substrate. Furthermore, Steigmann and Ogden (1997, 1999) generalized

* Corresponding author at: Department of Mechanical Engineering, Northwestern University, Evanston, IL 60208, USA. Tel.: +1 847 467 4528; fax: +1 847 491 4011.
E-mail address: j-qu@northwestern.edu (J. Qu).

0167-6636/$ - see front matter © 2012 Elsevier Ltd. All rights reserved.
http://dx.doi.org/10.1016/j.mechmat.2012.07.008

Gurtin–Murdoch model to account for the effects of intrinsic flexural resistance of surface/interface. Refinements to the general Gurtin–Murdoch framework (Gurtin and Murdoch, 1975) have also been made in recently years to account for, e.g., the interfacial incoherency (Wang and Pan, 1994), finite deformation of the interface (Nix and Gao, 1998), the three-dimensional nature and the Poisson's effects of the interface (Dingreville and Qu, 2008) and the effects of corrugation (Wang et al., 2010) of the surfaces/interfaces.

The elastic state of an inhomogeneity with prescribed eigenstrain (misfit) strains embedded in a foreign matrix is one of the most important problems in continuum mechanics. The problem is generally known as the Eshelby's problem because of his pioneering work (Eshelby, 1957, 1959), and is widely used in mechanics, material science and solid-state physics. It is considered the cornerstone of modern micromechanics (Mura, 1987; Qu and Cherkaoui, 2006). When the inhomogeneity size is in the nanometer scale, interfacial stress between the inhomogeneity and matrix can play a significant role. Thus, the original Eshelby's solution needs to be modified for nano-scale inhomogeneities to account for the effects of interfacial stresses. Using the Green's function approach, Sharma and Ganti (2004) and Sharma et al. (2003) obtained the modified Eshelby solution for a spherical inhomogeneity in an isotropic solid when the prescribed eigenstrain is dilatational. Tian and Rajapakse (2007) solved the same two-dimensional problem under arbitrary eigenstrain and remote loading using the Muskhelishvili's complex function method. Duan et al. (2005a,b,c) studied the stress concentration tensors of spherical inhomogeneities, and their effects on the effective elastic constants of composite materials consisting of nano-scale inhomogeneities, again assuming elastic isotropy for both the inhomogeneity and the matrix.

In summary, all the existing work assumes that the inhomogeneity is spherical, and both the inhomogeneity and the surrounding matrix are elastically isotropic. In many applications, most notably, precipitate strengthening in high strength alloys and embedded quantum dots, both the inhomogeneity (precipitate and quantum dot) and the surrounding matrix are anisotropic. Furthermore, the shape of the precipitate is typically non-spherical, and the eigenstrains are typically not pure dilatational. Therefore, it is necessary to obtain the elastic state of an inhomogeneity of arbitrary shape in an elastically anisotropic matrix subjected to an arbitrary eigenstrain field.

In this paper, we develop a variational formulation to study the problem of an inhomogeneity with arbitrary shapes and eigenstrains. Both the inhomogeneity and the surrounding matrix can be generally anisotropic. The solution is semi-analytical in that all the elastic field quantities are given explicitly in terms of polynomial functions whose coefficients can be solved from solving a system of linear algebraic equations. To illustrate the solution procedure, several examples are given. The validity and accuracy of the solution method are verified by comparing the numerical solutions with available analytical solutions in the isotropic case.

2. Problem statement

We consider an inhomogeneity Ω embedded in an otherwise homogeneous matrix of infinite extent. Assume that Ω is a singly-connected finite region of arbitrary shape, bounded by a smooth surface S with outward unit normal $\mathbf{n}$. Both the inhomogeneity and the matrix are elastic, and their elastic stiffness tensors are denoted by the fourth order tensors $\mathbf{C}^I$ and $\mathbf{C}^M$, respectively. Note that both $\mathbf{C}^I$ and $\mathbf{C}^M$ can be anisotropic. Further, we assume that the interface between the inhomogeneity and the matrix is coherent, i.e.,

$$[\mathbf{u}] = \mathbf{u}(S^+) - \mathbf{u}(S^-) = 0, \tag{1}$$

where $\mathbf{u}$ is the displacement field, and S^+ and S^- mean approaching the interface from the matrix side (+) and from the inhomogeneity side (−), respectively, see Fig. 1.

Let a uniform eigenstrain field $\boldsymbol{\varepsilon}^*$ be applied to the inhomogeneity. Our objective is to find the stress and strain fields caused by the applied eigenstrain. This elasticity problem for a conventional size inhomogeneity has been solved by Eshelby (1957, 1959). In this paper, we are interested in the case when the inhomogeneity is very small so that interfacial stress becomes non-negligible.

The interfacial excess energy density can be written as (Dingreville and Qu, 2008)

$$\Gamma = \Gamma_0 + \boldsymbol{\Gamma}^{(1)} : \boldsymbol{\varepsilon}^s + \frac{1}{2}\boldsymbol{\varepsilon}^s : \boldsymbol{\Gamma}^{(2)} : \boldsymbol{\varepsilon}^s, \tag{2}$$

where Γ_0, $\boldsymbol{\Gamma}^{(1)}$ and $\boldsymbol{\Gamma}^{(2)}$ are the intrinsic interfacial elasticity properties (Dingreville and Qu, 2008) that can be calculated once the material system is given (Dingreville and Qu, 2009). The interfacial strain can be computed from

$$\boldsymbol{\varepsilon}^s = \frac{1}{2}[\mathbf{P}\cdot(\nabla_s\mathbf{u}) + (\nabla_s\mathbf{u})^T\cdot\mathbf{P}], \tag{3}$$

where $\mathbf{P} = \mathbf{I} - \mathbf{n}\otimes\mathbf{n}$ is the projection tensor, $\mathbf{I}$ is the identity tensor, $\otimes$ represents a dyad, and the surface gradient is defined as $\nabla_s\mathbf{u} = \nabla\mathbf{u}\cdot\mathbf{P}$. The corresponding interfacial stress can be obtained from the interfacial excess energy from the Shuttleworth equation (Shuttleworth, 1950),

$$\boldsymbol{\Sigma}^s = \frac{\partial\Gamma}{\partial\boldsymbol{\varepsilon}^s} = \boldsymbol{\Gamma}^{(1)} + \boldsymbol{\Gamma}^{(2)} : \boldsymbol{\varepsilon}^s. \tag{4}$$

3. Weak form of the governing equations

To derive the governing equations, consider the potential energy of the system consisting of the inhomogeneity

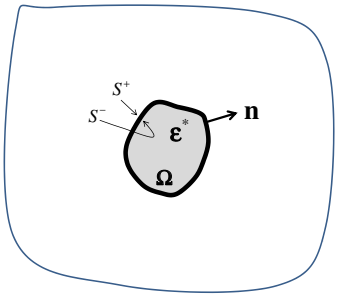

Fig. 1. An inhomogeneity in the matrix subjected to a uniform eigenstrain.

and the matrix. Since there are no applied forces, the potential energy of the system is the elastic strain energy

$$U = U_M + U_I + U_S, \tag{5}$$

where

$$U_M = \frac{1}{2}\int_{V_M} \boldsymbol{\sigma} : \boldsymbol{\varepsilon}\, dV, \quad U_I = \frac{1}{2}\int_{\Omega} \boldsymbol{\sigma} : (\boldsymbol{\varepsilon} - \boldsymbol{\varepsilon}^*)\, dV,$$
$$U_S = \int_S \Gamma\, dS \tag{6}$$

are the strain energy in the matrix, strain energy in the inhomogeneity and the interfacial excess energy on the inhomogeneity/matrix interface, respectively. In (6), V_M is the matrix domain, Ω is the inhomogeneity domain, and S is the inhomogeneity/matrix interface. Furthermore, we assume small strain deformation so that the strain tensor is related to the displacement field by

$$\boldsymbol{\varepsilon} = \frac{1}{2}[\nabla \mathbf{u} + (\nabla \mathbf{u})^T], \tag{7}$$

and the stress $\boldsymbol{\sigma}$ and strain $\boldsymbol{\varepsilon}$ are related through the Hooke's law,

$$\boldsymbol{\sigma} = \begin{cases} \mathbf{C}^I : (\boldsymbol{\varepsilon} - \boldsymbol{\varepsilon}^*) & \mathbf{x} \in \Omega \\ \mathbf{C}^M : \boldsymbol{\varepsilon} & \mathbf{x} \in V_M \end{cases}. \tag{8}$$

According to the minimum potential energy theorem, among all the kinematically admissible displacement fields, the true solution to the problem minimizes the potential energy, i.e.,

$$\delta U = \delta U_M + \delta U_I + \delta U_S = 0. \tag{9}$$

Here, any differentiable vector field that satisfies (1) and vanishes at infinity is a kinematically admissible displacement field. By using the divergence theorem, one can show that the Euler equations of (9) are the equilibrium equations at the interface (Gurtin and Murdoch, 1975)

$$\nabla \cdot \boldsymbol{\sigma} = \mathbf{0} \quad \text{in the matrix and in the inhomogeneity}, \tag{10}$$
$$\boldsymbol{\sigma} \cdot \mathbf{n} + \nabla_s \cdot (\boldsymbol{\Sigma}^s) = \mathbf{0} \quad \text{on the interface}. \tag{11}$$

Thus, (9) provides a weak form of the governing equations if a kinematically admissible displacement field is selected. However, since a kinematically admissible displacement field must satisfy (1), it is rather difficult to select such a field. So, for numerical solutions, we consider another form of the functional by introducing a Lagrangian multiplier $\boldsymbol{\lambda}$ to relax the kinematic constraint (1),

$$\Pi = U + \int_S \boldsymbol{\lambda} \cdot [\mathbf{u}]\, dS \quad \text{or} \quad \delta\Pi = \delta U + \delta \int_S \boldsymbol{\lambda} \cdot [\mathbf{u}]\, dS = 0. \tag{12}$$

The Euler equations corresponding to (12) include all the equilibrium equations (10) and (11), as well as the interfacial coherent condition (1). Using (12) as the weak form of the governing equation for numerical solution allows the use of independent trial functions in the matrix and the inhomogeneity.

One caveat in using (12) is the apparent ambiguity of computing the interfacial strain from (3). Since the trial function for the displacement fields in the matrix is different from that in the inhomogeneity, the resulting interfacial strain may differ depends on which displacement field is used. However, since the coherent condition (1) becomes an Euler equation, the solution procedure itself forces the two displacement fields to be the same on the interface. Therefore, regardless which field is used to calculate the interfacial strain, the end results are the same.

To illustrate the above, let us define the averages

$$\bar{u}^s \equiv \frac{1}{2}[\mathbf{u}(S^+) + \mathbf{u}(S^-)],$$
$$\bar{\boldsymbol{\varepsilon}}^s = \frac{1}{2}\left[\mathbf{P} \cdot (\nabla_s \bar{\mathbf{u}}^s) + (\nabla_s \bar{\mathbf{u}}^s)^T \cdot \mathbf{P}\right]. \tag{13}$$

If the displacement is continuous at the interface, then $\bar{u}^s = \mathbf{u}(S^+) = \mathbf{u}(S^-)$. Thus, the second of (13) reduces to (3) because $\mathbf{P}\cdot(\nabla_s \mathbf{u})$ involves only the in-plane components of the displacement $\mathbf{u}(S^+) = \mathbf{u}(S^-)$. Similarly, following (4) one may introduce

$$\bar{\boldsymbol{\Sigma}}^s = \boldsymbol{\Gamma}^{(1)} + \boldsymbol{\Gamma}^{(2)} : \bar{\boldsymbol{\varepsilon}}^s. \tag{14}$$

Now, by using the divergence theorem, the second of (12) can be transformed to

$$\begin{aligned}\delta\Pi = &-\int_\Omega (\nabla \cdot \boldsymbol{\sigma}) \cdot \delta\mathbf{u}\, dV - \int_{V^M} (\nabla \cdot \boldsymbol{\sigma}) \cdot \delta\mathbf{u}\, dV \\ &+ \int_S [\mathbf{u}] \cdot \delta\boldsymbol{\lambda}\, dS - \int_S (\boldsymbol{\sigma} \cdot \mathbf{n} + \nabla_s \cdot \boldsymbol{\Sigma}^s) \cdot \delta\bar{\mathbf{u}}^s\, dS \\ &+ \int_S (\boldsymbol{\lambda} - \bar{\boldsymbol{\sigma}} \cdot \mathbf{n}) \cdot \delta\mathbf{u}\, dS = \mathbf{0}\end{aligned} \tag{15}$$

where

$$\bar{\boldsymbol{\sigma}} \equiv \frac{1}{2}[\boldsymbol{\sigma}(S^+) + \boldsymbol{\sigma}(S^-)]. \tag{16}$$

Since $\delta\mathbf{u}$, $\delta\boldsymbol{\lambda}$ and $\delta\bar{\mathbf{u}}^s$ are arbitrary and independent, the Euler equations corresponding to (15) are

$$\nabla \cdot \boldsymbol{\sigma} = \mathbf{0} \quad \text{in the matrix and in the inhomogeneity}, \tag{17}$$
$$\boldsymbol{\sigma} \cdot \mathbf{n} + \nabla_s \cdot (\bar{\boldsymbol{\Sigma}}^s) = \mathbf{0} \quad \text{on the interface}, \tag{18}$$
$$[\mathbf{u}] = \mathbf{0} \quad \text{on the interface}, \tag{19}$$
$$\boldsymbol{\lambda} - \bar{\boldsymbol{\sigma}} \cdot \mathbf{n} = \mathbf{0} \quad \text{on the interface}. \tag{20}$$

Clearly, a solution that satisfies (15) must also satisfy (19), the continuity of displacement across the interface. Thus, this ensures that the end results are the same regardless whether $\mathbf{u}(S^+)$, or $\mathbf{u}(S^-)$ or $\bar{u}^s$ is used to compute the interfacial strain. Furthermore, (20) also indicates that the Lagrangian multiplier $\boldsymbol{\lambda}$ is nothing but the average traction on the interface. We note that since the traction is discontinuous across the inhomogeneity/matrix interface, the average traction differs from the traction on S^+ and S^-.

4. Solution procedures

When the interface is coherent and interfacial stress is neglected, the strain within the inhomogeneity is constant under homogeneous eigenstrain (at least for a class of shapes such as an ellipsoid). However, this is generally not true when the interface is endowed with separate material parameters. To solve the couple boundary value problem, some approximation schemes have to be adopted. A straightforward method is through expanding

the field quantities in the form of Taylor series (Moschovidis and Mura, 1975; Sendeckyj, 1967). In the present work, we adopt a similar approach by expanding the displacement field into polynomials. For convenience, we attach a Cartesian coordinal system $\mathbf{x} = (x_1, x_2, x_3)^T$ to the inhomogeneity, so that far away from the origin, i.e., $r = \|\mathbf{x}\| \to \infty$, all field quantities vanish.

Within the inhomogeneity, we postulate that the displacement field can be expressed as

$$\mathbf{u} = \sum_{m_1,m_2,m_3=0}^{N_1,N_2,N_3} \mathbf{a}_{m_1 m_2 m_3} x_1^{m_1} x_2^{m_2} x_3^{m_3} + \boldsymbol{\varepsilon}^* \cdot \mathbf{x}, \tag{21}$$

where $\boldsymbol{\varepsilon}^*$ is the prescribed eigenstrain on the inhomogeneity, and N_1, N_2 and N_3 are the upper limits of the summation for m_1, m_2 and m_3, respectively. For each given set of m_1, m_2 and m_3, $\mathbf{a}_{m_1 m_2 m_3}$ is a 1×3 vector whose components are unknown constants to be determined by the weak form of the governing Eq. (12). Clearly, there are $3 \times N_1 \times N_2 \times N_3$ unknown constants in (21). The accuracy of the numerical solution depends on the number of terms used in the expansion. In this work, the series was truncated when the coefficients of two additional terms in the expansion are less than 1% of those of the previous two terms.

For convenience, we introduce a shorthand notation (Wang and Pan, 1994) to denote an integer triplet m_1, m_2 and m_3 by its base letter with curly brackets, e.g., $\{m\} \Longleftrightarrow m_1, m_2, m_3$ and $\{N\} \Longleftrightarrow N_1, N_2, N_3$. This way, one may use $\mathbf{a}_{\{m\}}$ to denote $\mathbf{a}_{m_1 m_2 m_3}$. Eq. (21) can then be written as

$$\mathbf{u} = \sum_{\{m\}=0}^{\{N\}} \mathbf{a}_{\{m\}} x_1^{m_1} x_2^{m_2} x_3^{m_3} + \boldsymbol{\varepsilon}^* \cdot \mathbf{x}. \tag{22}$$

Making use of (21) in the second of (6) in conjunction with (7) and (8), one obtains

$$\delta U_I = \int_\Omega \boldsymbol{\sigma} : \delta\boldsymbol{\varepsilon}\, dV = \sum_{\{m\},\{p\}=0}^{\{N\}} \mathbf{a}_{\{m\}} \mathbf{K}^I_{\{m\}\{p\}} \delta\mathbf{a}_{\{p\}}, \tag{23}$$

where $\mathbf{K}^I_{\{m\}\{p\}}$ is a known constant 3×3 array that involves the integrals of polynomials over the inhomogeneity and the elastic stiffness tensor $\mathbf{C}^I$. We note that $\mathbf{K}^I_{\{m\}\{p\}}$ is symmetric and positive definite because of the positive definiteness of the stiffness tensor $\mathbf{C}^I$.

In the matrix, we can postulate that

$$\mathbf{u} = \sum_{\{m\}=0}^{\{N\}} \mathbf{b}_{\{m\}} x_1^{m_1} x_2^{m_2} x_3^{m_3} \|\mathbf{x}\|^{-2(m_1+m_2+m_3)}, \tag{24}$$

where $\mathbf{b}_{\{m\}}$ is an array of unknown constants to be determined. This functional form ensures that all the field quantities vanish at infinity. Making use of (24) in the first of (6) in conjunction with (7) and (8), one obtains

$$\delta U_M = \int_{V_M} \boldsymbol{\sigma} : \delta\boldsymbol{\varepsilon}\, dV = \sum_{\{m\},\{p\}=0}^{\{N\}} \mathbf{b}_{\{m\}} \mathbf{K}^M_{\{m\}\{p\}} \delta\mathbf{b}_{\{p\}}, \tag{25}$$

where $\mathbf{K}^M_{\{m\}\{p\}}$ is a known constant 3×3 array that involves the integrals of polynomials over the matrix and the elastic constants.

As noted earlier, to compute the interfacial strain from (3), either the displacement field in the matrix or in the inhomogeneity can be used. For convenience, we use the displacement in the matrix (24). Thus, it follows from using (24) in (3), one can compute

$$\begin{aligned}\delta U_S &= \int_S \delta\Gamma\, dS \\ &= \sum_{\{p\}=0}^{\{N\}} \delta\mathbf{b}_{\{p\}} \mathbf{F}^S_{\{p\}} + \sum_{\{m\},\{p\}=0}^{\{N\}} \delta\mathbf{b}_{\{p\}} \mathbf{K}^S_{\{p\}\{m\}} \mathbf{b}_{\{m\}},\end{aligned} \tag{26}$$

where $\mathbf{F}^S_{\{p\}}$ and $\mathbf{K}^S_{\{m\}\{p\}}$ are known constant 1×3 and 3×3 arrays that involve the integrals of polynomials over the inhomogeneity/matrix interface and the intrinsic interfacial elasticity tensors, $\boldsymbol{\Gamma}^{(1)}$ and $\boldsymbol{\Gamma}^{(2)}$.

Finally, variation of the Lagrange multiplier can be obtained by using (20)

$$\begin{aligned}\delta \int_S \boldsymbol{\lambda} \cdot [\mathbf{u}]\, dS = &\sum_{\{m\},\{p\}=0}^{\{N\}} \delta\mathbf{a}_{\{p\}} (\mathbf{L}^I_{\{p\}\{m\}} \mathbf{a}_{\{m\}} - \mathbf{H}^P_{\{p\}\{m\}} \mathbf{b}_{\{m\}}) \\ &- \sum_{\{m\},\{p\}=0}^{\{N\}} \delta\mathbf{b}_{\{p\}} \mathbf{H}^M_{\{p\}\{m\}} \mathbf{a}_{\{m\}} - \sum_{\{p\}=0}^{\{N\}} \delta\mathbf{a}_{\{p\}} \mathbf{F}^*_{\{p\}},\end{aligned} \tag{27}$$

where $\mathbf{L}^I_{\{m\}\{p\}}$, $\mathbf{H}^P_{\{p\}\{m\}}$ and $\mathbf{H}^M_{\{p\}\{m\}}$ are known constant 3×3 matrices that involve the integrals of polynomials over the inhomogeneity/matrix interface and the elastic stiffness tensors of the inhomogeneity and the matrix, respectively, and $\mathbf{F}^*_{\{p\}}$ is a known constant 1×3 vector that involves the eigenstrain and integrals of polynomials over the inhomogeneity/matrix interface and the elastic stiffness tensors of the inhomogeneity.

Substituting (23) into (25) and (27) into (12) yields

$$\begin{aligned}&\sum_{\{m\},\{p\}=0}^{\{N\}} \delta\mathbf{a}_{\{p\}} \left[\left(\mathbf{K}^I_{\{p\}\{m\}} + \mathbf{L}^I_{\{p\}\{m\}} \right) \mathbf{a}_{\{m\}} - \mathbf{H}^P_{\{p\}\{m\}} \mathbf{b}_{\{m\}} \right] \\ &+ \sum_{\{m\},\{p\}=0}^{\{N\}} \delta\mathbf{b}_{\{p\}} \left[\left(\mathbf{K}^M_{\{p\}\{m\}} + \mathbf{K}^S_{\{p\}\{m\}} \right) \mathbf{b}_{\{m\}} - \mathbf{H}^M_{\{p\}\{m\}} \mathbf{a}_{\{m\}} \right] \\ &+ \sum_{\{p\}=0}^{\{N\}} \left(\delta\mathbf{b}_{\{p\}} \mathbf{F}^S_{\{p\}} - \delta\mathbf{a}_{\{p\}} \mathbf{F}^*_{\{p\}} \right) = 0.\end{aligned} \tag{28}$$

Since $\delta\mathbf{a}_{\{p\}}$ and $\delta\mathbf{b}_{\{p\}}$ are arbitrary and independent, (28) leads to

$$\sum_{\{m\}=0}^{\{N\}} \left[\left(\mathbf{K}^I_{\{p\}\{m\}} + \mathbf{L}^I_{\{p\}\{m\}} \right) \mathbf{a}_{\{m\}} - \mathbf{H}^P_{\{p\}\{m\}} \mathbf{b}_{\{m\}} - \mathbf{F}^*_{\{p\}} \right] = 0, \quad \{p\} = 0, 1, \ldots, \{N\}, \tag{29}$$

$$\sum_{\{m\}=0}^{\{N\}} \left[\left(\mathbf{K}^M_{\{p\}\{m\}} + \mathbf{K}^S_{\{p\}\{m\}} \right) \mathbf{b}_{\{m\}} - \mathbf{H}^M_{\{p\}\{m\}} \mathbf{a}_{\{m\}} + \mathbf{F}^S_{\{p\}} \right] = 0, \quad \{p\} = 0, 1, \ldots, \{N\}, \tag{30}$$

This is a system of $6 \times N_1 \times N_2 \times N_3$ algebraic equations for the same number of unknown constants $\mathbf{a}_{\{m\}}$ and $\mathbf{b}_{\{m\}}$, for $\{m\} = 0, 1, \ldots, \{N\}$. The explicit expressions of $\mathbf{K}^I_{\{p\}\{m\}}$, $\mathbf{K}^M_{\{p\}\{m\}}$, $\mathbf{K}^S_{\{p\}\{m\}}$, $\mathbf{H}^P_{\{p\}\{m\}}$, $\mathbf{H}^M_{\{p\}\{m\}}$, $\{\mathbf{L}\}^{\mathbf{I}}_{\{\mathbf{p}\}\{\mathbf{m}\}}$, $\mathbf{F}^*_{\{p\}}$ and $\mathbf{F}^S_{\{p\}}$ are given in the appendix for a spherical inhomogeneity. Once this system of equations are solved, displacements fields in both the matrix and the inhomogeneity can be evaluated by substituting $\mathbf{a}_{\{m\}}$, $\mathbf{b}_{\{m\}}$ back to (22) and (24),

respectively. Some numerical examples will be given in the next section.

5. Numerical examples

As an example to illustrate the solution methodology developed in previous sections, we consider a spherical inhomogeneity of radius $R = 4$ nm embedded in an otherwise infinite solid. A Cartesian coordinate system is attached to the center of the inhomogeneity so that the inhomogeneity is given by

$$\Omega = \left\{ x_1, x_2, x_3; \sqrt{x_1^2 + x_2^2 + x_3^2} \leqslant R \right\}. \tag{31}$$

For convenience, a spherical coordinate system (r, θ, φ), see Fig. 2, is also introduced through

$$x_1 = r\sin\theta\cos\varphi, \quad x_2 = r\sin\theta\sin\varphi, \quad x_3 = r\cos\theta. \tag{32}$$

For simplicity, we further assume that the interfacial elasticity tensors are isotropic and given by (Dingreville and Qu, 2008; Gurtin and Murdoch, 1975)

$$\Gamma^{(1)}_{\alpha\beta} = \tau_0\delta_{\alpha\beta}, \quad \Gamma^{(2)}_{\alpha\beta\kappa\lambda} = \lambda^s\delta_{\alpha\beta}\delta_{\kappa\lambda} + \mu^s(\delta_{\alpha\kappa}\delta_{\beta\lambda} + \delta_{\alpha\lambda}\delta_{\beta\kappa}), \tag{33}$$

where $\tau_0 = 0.9108$ N/m, $\lambda^s = 6.8511$ N/m, $\mu^s = -0.3760$ N/m (Miller and Shenoy, 2000).

In what follows, we will consider two cases, (1) both the inhomogeneity and the matrix are elastically isotropic, and (2) both the inhomogeneity and the matrix are elastically cubic. The interfacial elasticity tensor above will be used for both cases.

5.1. Isotropic inhomogeneity and isotropic matrix with dilatational eigenstrain

Since this problem has been solved by Sharma and Ganti (2004) and Sharma et al. (2003), it provides a benchmark to validate our numerical solutions. To proceed, we assume that the isotropic elastic Young's and shear moduli for the inhomogeneity and the matrix are given by $\lambda^I = 50.66$ GPa, $\mu^I = 19.0$ GPa, $\lambda^M = 64.43$ GPa, and $\mu^M = 32.9$ GPa (Sharma and Ganti, 2002). The prescribed eigenstrain is dilatational $\varepsilon^*_{ij} = \varepsilon_0\delta_{ij}$, with $\varepsilon_0 = 0.01$.

Shown in Fig. 3 is the comparison of the radial displacement between the present solution and that of Sharma et al. (2003). The solutions presented in Fig. 3 were obtained using $N_1 = N_2 = N_3 = 3$ for the inhomogeneity and $N_1 = N_2 = N_3 = 7$ for the matrix. It is seen that the solution reproduces the existing result accurately.

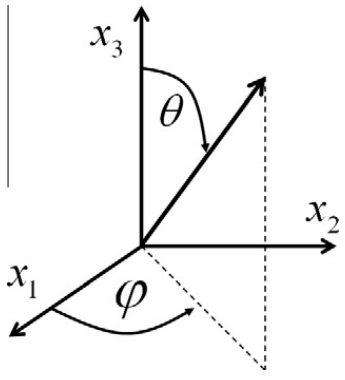

Fig. 2. A spherical coordinate system.

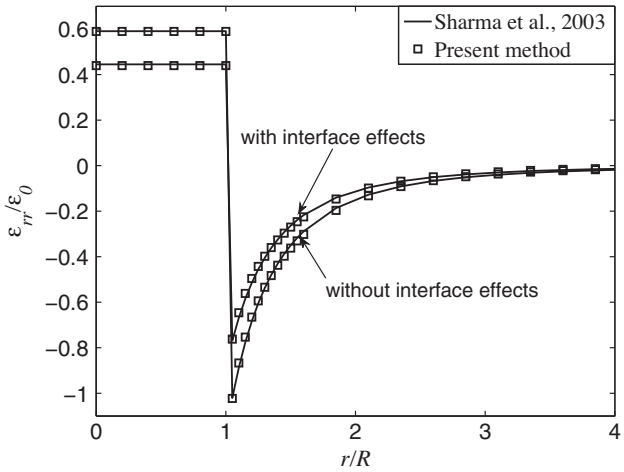

Fig. 3. Total radial strain ε_{rr} under dilatational eigenstrain. The solid lines are from Sharma et al. (2003), and the symbols are numerical solutions from this paper.

5.2. Anisotropic inhomogeneity and anisotropic matrix

Because of the material anisotropy, the problem is no longer spherically symmetric. Such anisotropic inhomogeneity problems have not been solved before when interfacial stress is considered. To demonstrate that the numerical method developed here is capable of handling material anisotropy, we select $C^I_{11} = 83.0$ GPa, $C^I_{12} = 45.0$ GPa, $C^I_{44} = 40.0$ GPa, $C^M_{11} = 118.0$ GPa, $C^M_{12} = 54.0$ GPa, and $C^M_{44} = 59.0$ GPa. For the numerical solutions, $N_1 = N_2 = N_3 = 4$ is used for the inhomogeneity, and $N_1 = N_2 = N_3 = 9$ for the matrix.

First, consider the case where the eigenstrain is purely dilatational, $\varepsilon^*_{ij} = \varepsilon_0\delta_{ij}$. The corresponding total radial strain ε_{rr} and hoop strain $\varepsilon_{\theta\theta}$ are plotted in Figs. 4 and 5, respectively. The solid and dashed lines represent, respectively, the solutions with and without considering interfacial stress.

Several observations can be made. First, it is seen that the total strain field inside the inhomogeneity is still a constant independent of the orientation, same as in isotropic materials. Second, the interfacial excess energy reduces the total strain inside the inhomogeneity by more than 20%. This is because the interface acts as a stiff shell to constrain the expansion of the inhomogeneity, thus reducing the stress concentration. Third, the strain in the $[1\,1\,0]$ and $[\bar{1}\,1\,0]$ directions are identical, as expected from the cubic symmetry under hydrostatic eigenstrain. Fourth, although the elastic anisotropic has no effect inside the inhomogeneity, the deformation in the matrix is orientation dependent. Finally, the effects of interface and elastic anisotropy become negligible about 2 diameters away from the inhomogeneity.

Next, consider a pure shear eigenstrain $\varepsilon^*_{ij} = \gamma_0(1 - \delta_{ij})$. The corresponding radial strain ε_{rr} and hoop strain $\varepsilon_{\theta\theta}$ are plotted in Figs. 6 and 7, respectively. The results show that,

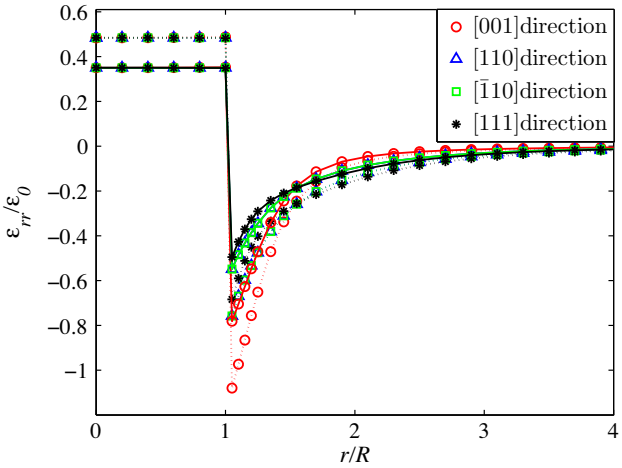

Fig. 4. Non-dimensional radial strain components ε_{rr} along different directions under dilatational eigenstrain. The solid and dashed lines represent, respectively, the solutions with and without considering interfacial stress.

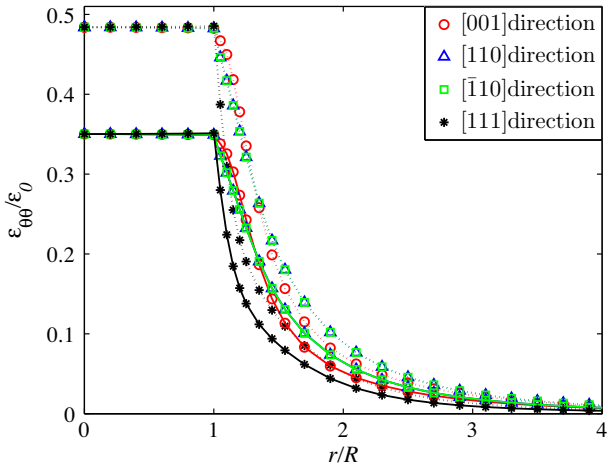

Fig. 5. Non-dimensional hoop strain components $\varepsilon_{\theta\theta}$ along different directions under hydrostatic eigenstrain. The solid and dashed lines represent, respectively, the solutions with and without considering interfacial stress.

in comparison to the previous example, the effects of interface are much more pronounced when the inhomogeneity is subjected to a shear eigenstrain. For example, the total strain fields in the $[1\,1\,0]$ and $[\bar{1}\,1\,0]$ directions are no longer anti-symmetric when the effects of interface is considered. Further, the interfacial stress does not lower the total strain magnitude consistently. In fact, it increases the total strain amplitude in the $(\bar{1}\,1\,0)$ direction. More importantly, the total strain inside the inhomogeneity becomes visibly non-uniform. This is particularly obvious for the hoop strain along the $[1\,1\,1]$ direction.

Once the displacement and strain fields are known, the corresponding stress fields can be computed using the Hooke's law. When interfacial stress is considered, the traction across the inhomogeneity/matrix interface is no longer continuous. This is illustrated in Figs. 8 and 9, where the distribution of σ_{rr} along different radial directions is

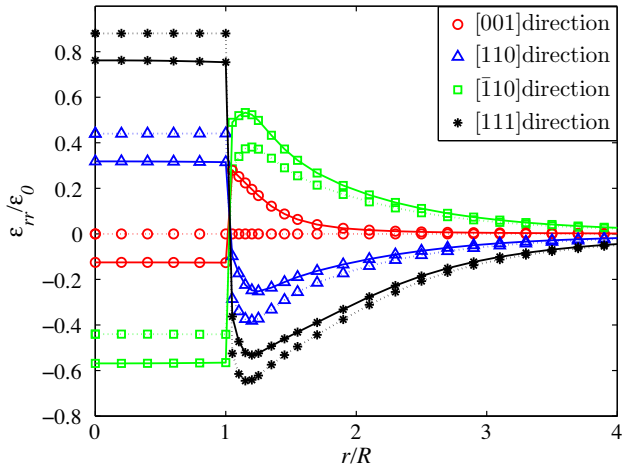

Fig. 6. Non-dimensional radial strain ε_{rr} along different directions under pure shear eigenstrain. The solid and dashed lines represent, respectively, the solutions with and without considering interfacial stress.

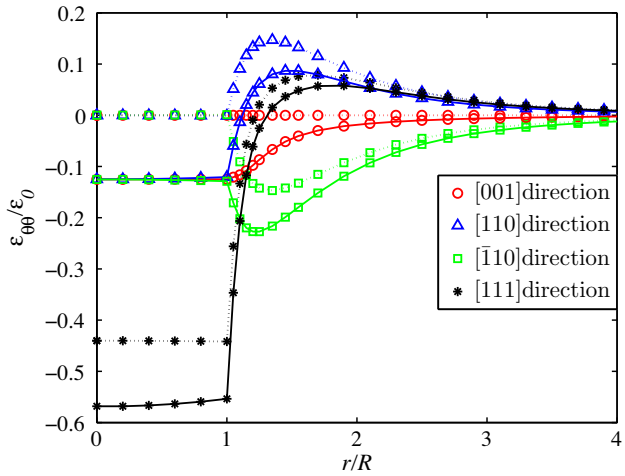

Fig. 7. Non-dimensional hoop strain $\varepsilon_{\theta\theta}$ along different directions under pure shear eigenstrain. The solid and dashed lines represent, respectively, the solutions with and without considering interfacial stress.

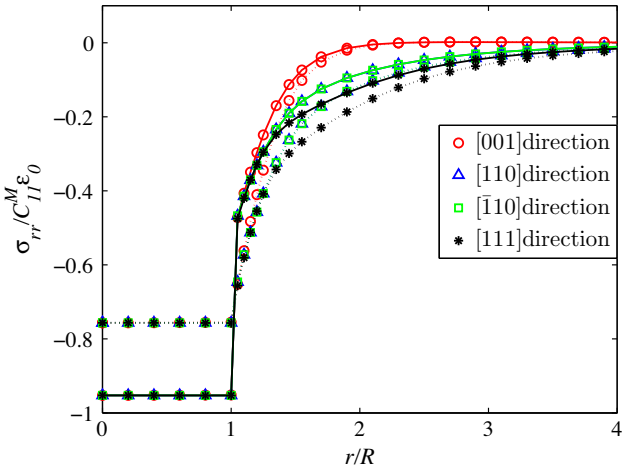

Fig. 8. Radial stress σ_{rr} along different directions under dilatational eigenstrain. The solid and dashed lines represent, respectively, the solutions with and without considering interfacial stress.

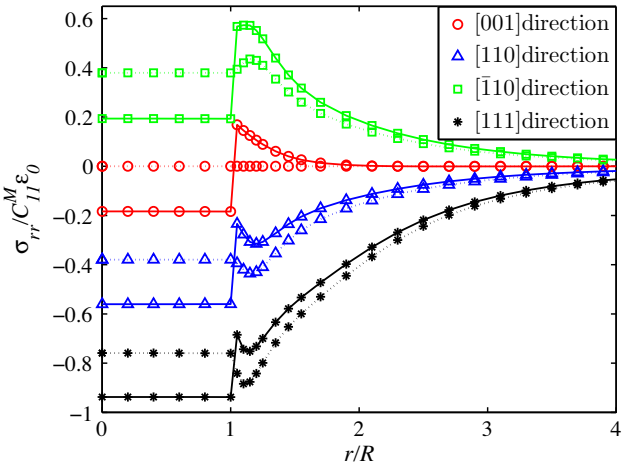

Fig. 9. Radial stress σ_{rr} along different directions under pure shear eigenstrain. The solid and dashed lines represent, respectively, the solutions with and without considering interfacial stress.

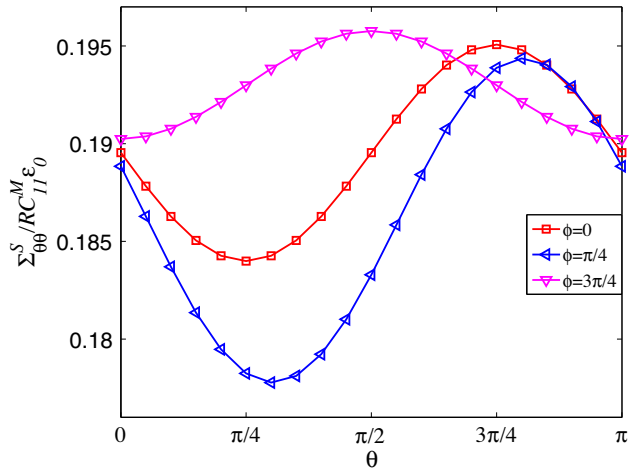

Fig. 10. Interfacial stress $\Sigma^s_{\theta\theta}$ under pure shear eigenstrain $\left(\Sigma^s_{\theta\theta}=\Sigma^s_{\varphi\varphi}\right)$.

plotted. The discontinuities at the interface are clearly seen.

It follows from (11) that the jump in the interfacial traction across the interface is given by $\nabla_s\cdot(\boldsymbol{\Sigma}^s)$. To understand the traction jumps, the interfacial stress $\Sigma^s_{\theta\theta}$, $\Sigma^s_{\varphi\varphi}$, and $\Sigma^s_{\varphi\theta}$ have been obtained. It can be shown analytically from (18) that $\Sigma^s_{\theta\theta}$ should be a constant under dilatational eigenstrain. Our numerical results do confirm this. Under pure shear eigenstrain, the interfacial stresses are no longer constants. Fig. 10 shows $\Sigma^s_{\theta\theta}$ along the azimuthal direction under pure shear eigenstrains.

6. Conclusion

In this paper, we have developed a variational formulation to solve the general anisotropic nano-inhomogeneity problem incorporating the interfacial stress. We demonstrated that the method is robust and accurate, and applicable to non-spherical and anisotropic inhomogeneities, as well as anisotropic matrix. As an example, we studied a spherical nano-inhomogeneity with elastic cubic symmetry. It is found that the interface stress lowers the strain and stress fields when the eigenstrain is dilatational. This is no longer the case when a pure shear eigenstrain field is applied.

Acknowledgements

The work was supported in part by NSF (CMMI 0726286).

Appendix A

For simplicity, the following notations are employed here,

$$X_{\{m\}}=x_1^{m_1}x_2^{m_2}x_3^{m_3},\quad \widetilde{X}_{\{m\}}=X_{\{m\}}\|\mathbf{x}\|^{\alpha_{\{m\}}},\qquad \alpha_{\{m\}}=-2(m_1+m_2+m_3) \tag{A.1}$$

and

$$\mathbf{C_{IJ}}=\begin{pmatrix}\mathbf{I}\\ \mathbf{J}\end{pmatrix}_C=\begin{pmatrix}i_1 & i_2 & i_3\\ j_1 & j_2 & j_3\end{pmatrix}_C=\begin{bmatrix}C_{i_1j_1} & C_{i_1j_2} & C_{i_1j_3}\\ C_{i_2j_1} & C_{i_2j_2} & C_{i_2j_3}\\ C_{i_3j_1} & C_{i_3j_2} & C_{i_3j_3}\end{bmatrix}, \tag{A.2}$$

where $\mathbf{I}=\{i_1\ i_2\ i_3\}$ and $\mathbf{J}=\{j_1\ j_2\ j_3\}$ are vectors that can take **1**, **2**, **3** corresponding [1 6 5], [6 2 4] and [5 4 3], respectively. It should be mentioned that the boldface $\mathbf{C_{IJ}}$ here is a 3×3 matrix, while the italic C_{ij} is one of the components of the 6×6 stiffness matrix.

The matrix involved in (23) can be expressed as

$$\mathbf{K}^I_{\{p\}\{m\}IJ}=\mathbf{C}^I_{\mathbf{IJ}}:\boldsymbol{\beta}^I, \tag{A.3}$$

where

$$\boldsymbol{\beta}^I_{ij}=\int_\Omega X_{\{m\}}X_{\{p\}}\frac{m_i}{x_i}\frac{p_j}{x_j}\,dV. \tag{A.4}$$

The matrix in (25) is written as

$$\mathbf{K}^M_{\{p\}\{m\}IJ}=\mathbf{C}^M_{\mathbf{IJ}}:\boldsymbol{\beta}^M, \tag{A.5}$$

where

$$\begin{aligned}\boldsymbol{\beta}^M_{ij}&=\tilde{\boldsymbol{\beta}}_{ij}+\left(m_i\alpha_{\{p\}}\boldsymbol{\beta}^*_{ij}+p_j\alpha_{\{m\}}\boldsymbol{\beta}^*_{ji}\right)+\alpha_{\{m\}}\alpha_{\{p\}}\hat{\boldsymbol{\beta}}_{ij}\\ \tilde{\boldsymbol{\beta}}_{ij}&=\textstyle\int_{V_M}\widetilde{X}_{\{m\}}\widetilde{X}_{\{p\}}\frac{m_i}{x_i}\frac{p_j}{x_j}\,dV\\ \boldsymbol{\beta}^*_{ij}&=\textstyle\int_{V_M}\widetilde{X}_{\{m\}}\widetilde{X}_{\{p\}}\frac{x_j}{x_i}\frac{1}{\|\mathbf{x}\|^2}\,dV\\ \hat{\boldsymbol{\beta}}_{ij}&=\textstyle\int_{V_M}\widetilde{X}_{\{m\}}\widetilde{X}_{\{p\}}\frac{x_ix_j}{\|\mathbf{x}\|^4}\,dV\end{aligned}. \tag{A.6}$$

The matrix in (26) is

$$\begin{aligned}\mathbf{K}^S_{\{p\}\{m\}IJ}&=\int_S\widetilde{X}_{\{m\}}\widetilde{X}_{\{p\}}\boldsymbol{\Gamma}^*_{IJ}\,dS,\\ \mathbf{F}^S_{\{p\}I}&=\tau_0\int_S\widetilde{X}_{\{p\}}\left(T_{2I}\widetilde{V}_2^{\{p\}}+T_{3I}\widetilde{V}_3^{\{p\}}\right)dS,\end{aligned} \tag{A.7}$$

where

$$\begin{aligned}\boldsymbol{\Gamma}^*_{ij}=&\left(K^S\mathbf{T}_{2i}\mathbf{T}_{2j}+\mu^S\mathbf{T}_{3i}\mathbf{T}_{3j}\right)\widetilde{V}_2^{\{m\}}\widetilde{V}_2^{\{p\}}\\ &+\left(K^S\mathbf{T}_{3i}\mathbf{T}_{3j}+\mu^S\mathbf{T}_{2i}\mathbf{T}_{2j}\right)\widetilde{V}_3^{\{m\}}\widetilde{V}_3^{\{p\}}\\ &+\left(\lambda^S\mathbf{T}_{2i}\mathbf{T}_{3j}+\mu^S\mathbf{T}_{3i}\mathbf{T}_{2j}\right)\widetilde{V}_2^{\{m\}}\widetilde{V}_3^{\{p\}}\\ &+\left(\lambda^S\mathbf{T}_{3i}\mathbf{T}_{2j}+\mu^S\mathbf{T}_{2i}\mathbf{T}_{3j}\right)\widetilde{V}_3^{\{m\}}\widetilde{V}_2^{\{p\}},\end{aligned} \tag{A.8}$$

$$\widetilde{V}_i^{\{m\}} = \mathbf{T}_{ij} V_j^{\{m\}}, \tag{A.9}$$

$$V^{\{m\}} = \left[\frac{m_1}{x_1} + \alpha_{\{m\}} \frac{x_1}{\|\mathbf{x}\|^2} \frac{m_2}{x_2} + \alpha_{\{m\}} \frac{x_2}{\|\mathbf{x}\|^2} \frac{m_3}{x_3} + \alpha_{\{m\}} \frac{x_3}{\|\mathbf{x}\|^2} \right]. \tag{A.10}$$

In the above, $\mathbf{T}$ is the coordinate transform matrix. For example, in the spherical coordinate system (r, θ, φ), we can write

$$\mathbf{T} = \begin{bmatrix} \sin\theta\cos\varphi & \sin\theta\sin\varphi & \cos\theta \\ \cos\theta\cos\varphi & \cos\theta\sin\varphi & -\sin\theta \\ -\sin\varphi & \cos\varphi & 0 \end{bmatrix}. \tag{A.11}$$

Moreover,

$$\mathbf{L}^I_{\{p\}\{m\}IJ} = \mathbf{C}^I_{\mathbf{IJ}} : \xi^M + \mathbf{C}^I_{\mathbf{JI}} : \xi^P, \tag{A.12}$$

$$\mathbf{H}^M_{\{p\}\{m\}IJ} = \mathbf{C}^I_{\mathbf{IJ}} : \hat{\xi}^M, \quad \mathbf{H}^P_{\{p\}\{m\}IJ} = \mathbf{C}^I_{\mathbf{JI}} : \hat{\xi}^P, \tag{A.13}$$

$$\mathbf{F}^*_{\{p\}I} = \mathbf{E}^P_I : \boldsymbol{\varepsilon}^*, \tag{A.14}$$

where

$$\xi^M_{ij} = \int_S X_{\{p\}} X_{\{m\}} n_i \frac{m_j}{x_j}\, dS, \quad \xi^P_{ij} = \int_S X_{\{p\}} X_{\{m\}} n_i \frac{p_j}{x_j}\, dS, \tag{A.15}$$

$$\hat{\xi}^M_{ij} = \int_S \widetilde{X}_{\{p\}} X_{\{m\}} n_i \frac{m_j}{x_j}\, dS, \quad \hat{\xi}^P_{ij} = \int_S \widetilde{X}_{\{m\}} X_{\{p\}} n_i \frac{p_j}{x_j}\, dS, \tag{A.16}$$

$$\mathbf{E}^P_{IJK} = \mathbf{C}^I_{\mathbf{JI}} : \boldsymbol{\eta}^P_K, \tag{A.17}$$

$$\left(\boldsymbol{\eta}^P_k\right)_{ij} = \int_S X_{\{p\}} n_i \frac{p_j}{x_j} x_k\, dS. \tag{A.18}$$

References

Ashby, M.F., Ferreira, P.J.S.G., Schodek, D.L., 2009. Nanomaterials, Nanotechnologies and Design: An Introduction for Engineers and Architects. Butterworth-Heinemann, Amsterdam, Boston.

Daw, M.S., Foiles, S.M., Baskes, M.I., 1993. The embedded-atom method: a review of theory and applications. Mater. Sci. Rep. 9, 251–310.

Dingreville, R., Qu, J., 2009. A semi-analytical method to estimate interface elastic properties. Comput. Mater. Sci. 46, 83–91.

Dingreville, R., Qu, J.M., 2008. Interfacial excess energy, excess stress and excess strain in elastic solids: planar interfaces. J. Mech. Phys. Solids 56, 1944–1954.

Dingreville, R., Qu, J.M., Cherkaoui, M., 2005. Surface free energy and its effect on the elastic behavior of nano-sized particles, wires and films. J. Mech. Phys. Solids 53, 1827–1854.

Duan, H.L., Wang, J., Huang, Z.P., Karihaloo, B.L., 2005a. Eshelby formalism for nano-inhomogeneities. Proc. R. Soc. A Math. Phys. 461, 3335–3353.

Duan, H.L., Wang, J., Huang, Z.P., Karihaloo, B.L., 2005b. Size-dependent effective elastic constants of solids containing nano-inhomogeneities with interface stress. J. Mech. Phys. Solids 53, 1574–1596.

Duan, H.L., Wang, J., Huang, Z.P., Luo, Z.Y., 2005c. Stress concentration tensors of inhomogeneities with interface effects. Mech. Mater. 37, 723–736.

Eshelby, J.D., 1957. The determination of the elastic field of an ellipsoidal inclusion, and related problems. Proc. R. Soc. Lond. Ser. A 241, 376–396.

Eshelby, J.D., 1959. The elastic field outside an ellipsoidal inclusion. Proc. R. Soc. Lond. Ser. A 252, 561–569.

Gurtin, M.E., Murdoch, A.I., 1975. A continuum theory of elastic material surfaces. Arch. Ration. Mech. Anal. 57, 291–323.

Gurtin, M.E., Weissmuller, J., Larche, F., 1998. A general theory of curved deformable interfaces in solids at equilibrium. Philos. Mag. A 78, 1093–1109.

He, J., Lilley, C.M., 2008. Surface stress effect on bending resonance of nanowires with different boundary conditions. Appl. Phys. Lett., 93.

Miller, R.E., Shenoy, V.B., 2000. Size-dependent elastic properties of nanosized structural elements. Nanotechnology 11, 139–147.

Moschovidis, Z.A., Mura, T., 1975. 2-Ellipsoidal inhomogeneities by equivalent inclusion method. J. Appl. Mech. ASME 42, 847–852.

Mura, T., 1987. Micromechanics of Defects in Solids, second rev. ed. Kluwer Academic Publishers, Dordrecht, Netherlands.

Nix, W.D., Gao, H.J., 1998. An atomistic interpretation of interface stress. Scr. Mater. 39, 1653–1661.

Qu, J., Cherkaoui, M., 2006. Fundamentals of Micromechanics of Solids. Wiley, Hoboken, New Jersey.

Sendeckyj, G.P., 1967. Ellipsoidal Inhomegeneity Problem. PhD thesis, Northwestern University.

Sharma, P., Ganti, S., 2002. Interfacial elasticity corrections to size-dependent strain-state of embedded quantum dots. Phys. Status Solidi B 234, R10–R12.

Sharma, P., Ganti, S., 2004. Size-dependent Eshelby's tensor for embedded nano-inclusions incorporating surface/interface energies. J. Appl. Mech. ASME 71, 663–671.

Sharma, P., Ganti, S., Bhate, N., 2003. Effect of surfaces on the size-dependent elastic state of nano-inhomogeneities. Appl. Phys. Lett. 82, 535–537.

Shuttleworth, R., 1950. The surface tension of solids. Proc. R. Soc. A 63, 444–457.

Steigmann, D.J., Ogden, R.W., 1997. Plane deformations of elastic solids with intrinsic boundary elasticity. Proc. R. Soc. Lond. A Mat. 453, 853–877.

Steigmann, D.J., Ogden, R.W., 1999. Elastic surface-substrate interactions. Proc. R. Soc. Lond. A Mat. 455, 437–474.

Tian, L., Rajapakse, R.K.N.D., 2007. Analytical solution for size-dependent elastic field of a nanoscale circular inhomogeneity. J. Appl. Mech. ASME 74, 568–574.

Wang, T.C., Pan, W.K., 1994. Mechanical modeling of grain-boundary sliding of polycrystals. Model. Simul. Mater. Sci. 2, 739–754.

Wang, Y., Weissmuller, J., Duan, H.L., 2010. Mechanics of corrugated surfaces. J. Mech. Phys. Solids 58, 1552–1566.

Zhao, X.J., Rajapakse, R.K.N.D., 2009. Analytical solutions for a surface-loaded isotropic elastic layer with surface energy effects. Int. J. Eng. Sci. 47, 1433–1444.